DETERMINATION OF THE IMPACT OF WIND POWER GENERATION ON THE STEADY-STATE VOLTAGE STABILITY OF DISTRIBUTION SYSTEMS

L. Mariotto, H. Pinheiro, G. Cardoso Junior, M.R. Muraro, I.W. Jaskulski
Centro de Tecnologia – Universidade Federal de Santa Maria
Santa Maria – Rio Grande do Sul – Brasil
mariotto@ct.ufsm.br, humberto@ctlab.ufsm.br, ghendy@smail.ufsm.br, matiasmuraro@gmail.com, igorwj@gmail.com

***Abstract* – This paper presents a method to evaluate the impact of wind power generation on the steady-state voltage stability of distribution power system. The basic requirements and the power capabilities limits of the wind turbine and converters are analyzed. It is demonstrated that the wind power capability limits can impose operational restrictions to the power system voltage stability limits. The methodology was first applied on a simple two-bus power system and it is shown that the results are very close to those obtained by using an analytical solution. The impact on voltage stability is analyzed by plotting the *P-Q* curves for different operation scenarios of wind power generation. Then, the power system *P-Q* curves are plotted considering the capability curves of wind turbines and it can be seen that an effective contribution of wind power to the voltage stability can be achieved by enlarging his reactive power region of operation.**

***Keywords* - *P-V* curves, *P-Q* curves, Voltage collapse, Voltage stability region, Wind power generation, Wind turbine power capability limits.**

I. INTRODUCTION

Nowadays, it is very common to find renewable energy resources, connected to distribution systems. The wind power has been an excellent alternative resource for distributed generation because it requires short installation time and causes low environment impact. By analyzing the wind turbines evolution in the last twenty years, it may be noticed a trend of growing rated power. This trend is driven by the reduction of wind turbine final costs. Rated power of modern wind turbines can exceed 5 MW. These turbines require static converters between the generator and the grid. The generators and converters are usually designed to operate at low voltages (<1kV) due to technical and economical reasons. As a result, high current levels, generally reaching units of kA, have to be managed and this can be a concern in terms of semiconductor devices selection, filter sizes, current and voltage harmonics emissions.

The impact of distributed generation on voltage distribution levels has been addressed in literature [1-2]. The majority of this works deals with the determination of the maximum active and reactive power that is possible to be connected on a system load bus, until the voltage at that bus reaches the voltage collapse point. It is done by the traditional *P-V* and *Q-V* curves methods, reported in many references as [3-5]. Static techniques are very useful to determine the load margin or how close the actual system operating state is from the point of voltage collapse point. Distribution system operators must know the maximum permissible loading at each bus, so that the voltages remain within the acceptable ranges, without causing any trouble or hazard to the equipments.

The method proposed in this paper determines this information by defining the limit regions for secure voltage operation in the *P-Q* plane, considering the basic requirements and the power capabilities limits of the wind turbine and converters. These regions give all the possible active and reactive power combinations in which each bus of the system can operate. It is carried out by using the DIgSILENT® Programming Language (DPL), which uses similar syntax to the C++ and is an internal programming language of the software DIgSILENT® Power Factory. To validate the developed program, an analytical method is performed [3]. In this reference, the author presents an analytical form to find the boundary of the voltage stability region in *P-Q* plane.

Initially, the proposed method was applied on a simple system with wind power generation represented by a direct drive synchronous generator. The results obtained from analytical solution and the computational method are very close. Finally, the computational method is applied on a distribution system considering four different scenarios of wind power operation modes. The power capabilities limits of wind turbines and converters are analyzed simultaneously with the power system voltage stability limit.

II. BASIC REQUIREMENTS AND CAPABILITIES LIMITS OF WIND TURBINES

Reference [6] selected six grid codes for wind turbines connected to the grid. The basics requirements summarized are from Canada, Denmark, Germany, Ireland, Scotland and United Kingdom. The most restringing wind power connection requirements were defined considering the following characteristics: voltage control, quality of voltage, power factor requirements, power curtailment, frequency and flicker. The operation limits of active and reactive power, considering the most restringing requirements of those six countries, are showed in Figure 1.

The region illustrated by gray rectangle in Figure 1 can be altered to increase the limits of reactive power when the wind velocity is to low to produce active power. Wind turbines that can operate at the power region defined in Figure 1 will satisfy all grid codes considered.

Wind Turbines can be used as voltage regulators and control the reactive power at the Point of Common Coupling (PCC) in order to keep the voltage within the limits and avoid voltage stability problems.

In order to achieve these requirements, the semiconductor devices, the DC bus voltage as well as the filter reactance

must be appropriately selected [7]. In the following section, these issues are addressed.

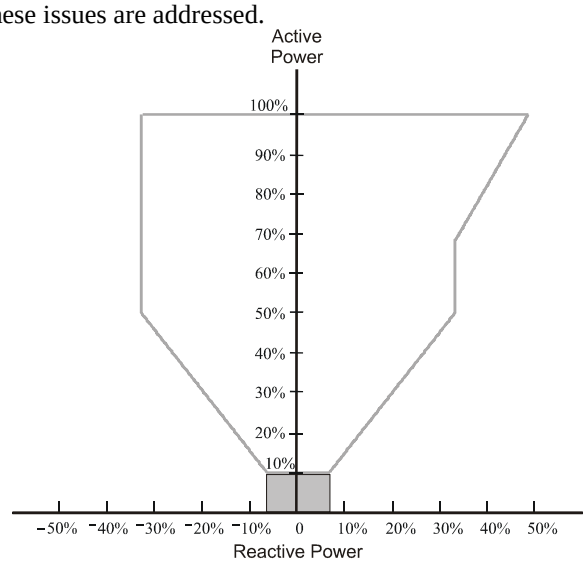

Fig. 1. The most restringing requirements for active and reactive power.

A. Thermal Limit

The operation of semiconductor devices results in losses, which are proportional to conduction current and the on-state saturation voltage. Thus, for a given output voltage, the output power is limited by maximum current I_{lim} supported by semiconductor devices. The thermal limit of the three-phase converter imposes limits in the active and reactive power that can be expressed as:

$$S^2 = P^2 + Q^2 = \left(3V_g I_{\lim}\right)^2 \qquad (1)$$

Where:

S, P and Q are apparent, active and reactive power and Vg is the grid voltage at the PCC.

Figure 2 shows the limits of the active and reactive power of a three-phase converter connected to the grid with semiconductor devices limited by I_{lim} = 1.2 p.u. and the grid voltage V_g changing from 0.2 p.u. to 1.2 p.u..

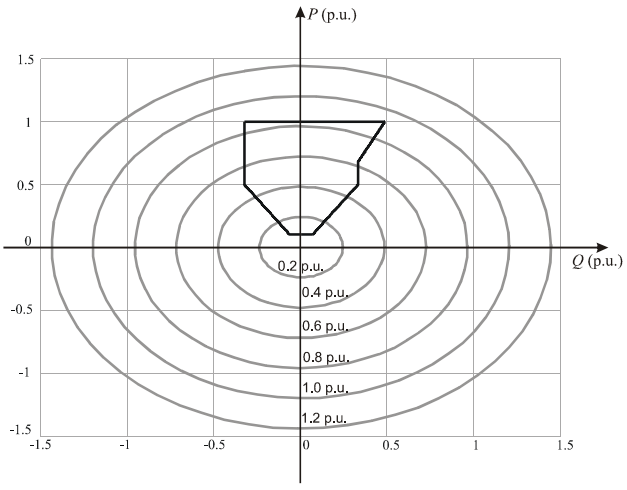

Fig. 2. Limits of *P* and *Q* as function of V_g.

B. DC Bus Voltage Limits

The limits of *P* and *Q* of the converter connected to grid are function of converter output voltage V_i, the voltage grid V_g and the total reactance *X* (which is the sum of filter and grid reactance at the PCC), the resistance can be neglected. The relation between those powers and these voltages is given in [7]:

$$P^2 + \left(Q + \frac{3V_g^2}{X}\right)^2 = \left(3\frac{V_g V_i}{X}\right)^2 \qquad (2)$$

Note that V_i is proportional to V_{dc} and the modulation strategy. The *P*-*Q* phasor diagram that describes (2) is showed in Figure 3. All the circumferences are traced with radius $\left(\frac{3V_g V_i}{X}\right)$, center C $\left(-\frac{3V_g^2}{X}, 0\right)$.

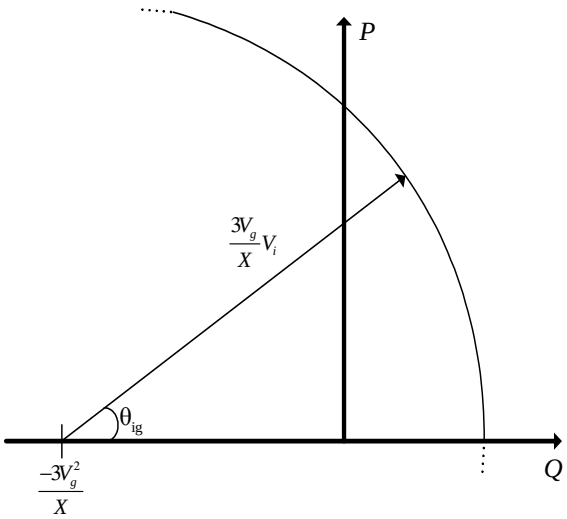

Fig. 3. *P* - *Q* Phasor diagram.

Figure 4 shows the operation limits of a three-phase converter when V_{dc} is changed. It was considered V_g = 1.0 p.u., *X* = 0.5 p.u. and V_i in the range of 1.0 p.u. to 1.5 p.u..

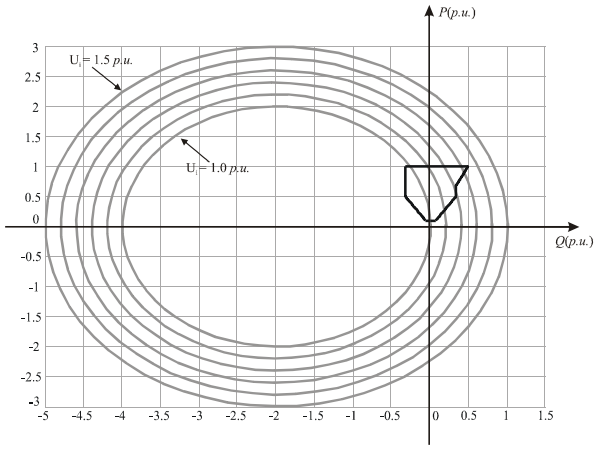

Fig. 4. Limits of *P* and *Q* as function of V_i.

C. Power Limit due to the Filter

Similarly to V_{dc}, the filter reactance limits *P* and *Q*. Figure 5 shows the operation limits with different values of filter reactance's. V_g and V_i remain constant at 1.00 p.u. and 1.20 p.u. , respectively, while *X* has been changed from 0.30 p.u. to 1.0 p.u..

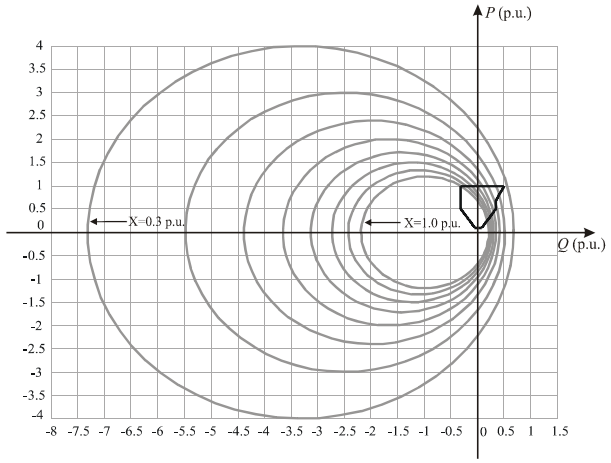

Fig. 5. Limits of *P* and *Q* as function of *X*.

It can be seen on Figure 5 that an important factor that limit the use of the converter as a reactive power compensator is the reactance *X*. It imposes limitations to the operation converter for values greater than 0.30 p.u..

III. DERIVING *P-V* AND *P-Q* CURVES

To clarify the proceedings adopted latter to derive the *P-Q* boundary stability region, it will be first considered a simple system, as shown in Figure 6.

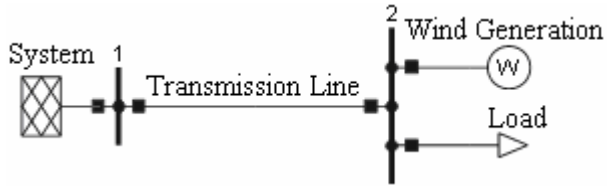

Fig. 6. A two-bus simplified power system.

The equations which give the relations between the voltages and the active and reactive power delivery on the load bus 2 of the system of Figure 6 can be written as:

$$P_2 + \left[\frac{AV_2^2}{B}\right]\cos(\gamma) = \left[\frac{V_1V_2}{B}\right]\cos(\beta-\theta) \quad (3)$$

$$P_2 tg\phi + \left[\frac{AV_2^2}{B}\right]\sin(\gamma) = \left[\frac{V_1V_2}{B}\right]\sin(\beta-\theta) \quad (4)$$

Where:

$\vec{A} = A\angle\alpha$ and $\vec{B} = B\angle\beta$ are the generalized circuit constants of the π equivalent model of the transmission line.

$P_2 =$ Active power at the load bus

$Q_2 = P_2 tg\phi$ = Reactive power at the load bus

$\vec{V}_1 = V_1\angle\theta_1$ = Voltage at the swing bus

$\vec{V}_2 = V_2\angle\theta_2$ = Voltage at the load bus

$\theta = \theta_1 - \theta_2$

$\gamma = \beta - \alpha$

Taking separately the square of equations (3) and (4) and adding them to eliminate θ, the resulting equation becomes a bi-quadratic form, where the voltage at bus 2 is the variable to be analyzed:

$$\left[\frac{A}{B}\right]^2 V_2^4 + \left[\left(\frac{2AP_2}{B}\right)(\cos\gamma + tg\phi\sin\gamma) - \left(\frac{V_1}{B}\right)^2\right]V_2^2 + P_2^2(1+tg^2\phi) = 0 \quad (5)$$

Equation (5) can be rewritten as:

$$aV_2^4 + bV_2^2 + c = 0 \quad (6)$$

Where:

$$a = \left[\frac{A}{B}\right]^2 \quad (7)$$

$$b = \frac{2ABP_2(\cos\gamma + tg\phi\sin\gamma) - V_1^2}{B^2} \quad (8)$$

$$c = P_2^2(1+tg^2\phi) \quad (9)$$

The solution of (6) is:

$$V_2^2 = \frac{-b \pm \sqrt{b^2-4ac}}{2a} \quad (10)$$

Only positive solutions for V_2 are of interest. Equation (10) gives the magnitude of the voltage V_2 as follows:

$$V_2 = \sqrt{\frac{-b \pm \sqrt{b^2-4ac}}{2a}} \quad (11)$$

Denoting the two solutions of (11) as V_2^1 and V_2^2 it is interesting to observe that when $(b^2-4ac)=0$, $V_2^1 = V_2^2 = V_2^{cr}$. The two equilibrium states becomes one. Therefore it is the critical operating point, and V_2^{cr} is the critical voltage.

A. P-V Curves Simulation

Suppose the three-phase single circuit, 345 kV and 450 km long transmission line given in reference [3]. The series impedance per phase is $\vec{z} =$ (0.0298 + j0.2849) Ω/km and the shunt admittance to ground is $\vec{y} =$ j3.9888 x 10-6 S/km.

The values of $\vec{A}$ and $\vec{B}$ constants that represent a π equivalent model of the transmission line can be addressed in [8]. *P-V* curves for different load power factors are shown in Figure 7, obtained with simulations using DIgSILENT® programming Language.

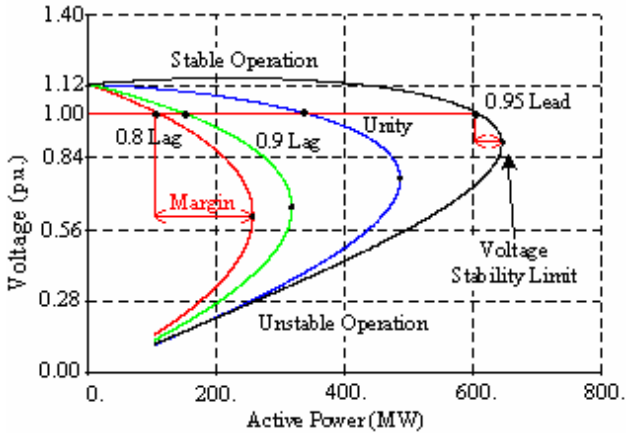

Fig. 7. *P-V* Curves for bus 2 at 1st and 4th quadrants.

It is shown in Figure 8 the *P-V* curves for different load power factors, in a special case, where the wind power generation produces more active power than the local load active power demand. Since the wind power in this case is a *P-Q* bus, high reverse active power flowing from the wind generator to the system can produce the voltage collapse on the local bus.

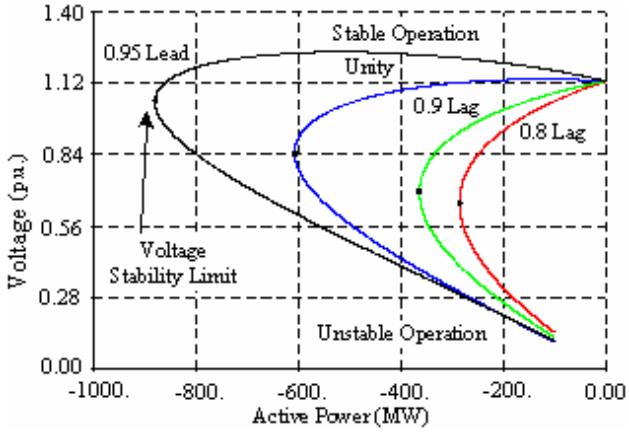

Fig. 8. *P-V* Curves for bus 2 at 2nd and 3rd quadrants.

B. Analytical solution

The critical equilibrium point is obtained from condition $(b^2 - 4ac) = 0$ on (11), and then it can be written as:

$$a'P_2^2 + b'P_2 + c' = 0 \qquad (12)$$

Where:

$$a' = 4[AB]^2\left[(\cos\gamma + tg\phi\sin\gamma)^2 - \left(1 + tg^2\phi\right)\right] \qquad (13)$$

$$b' = -4\left(ABV_1^2\right)(\cos\gamma + tg\phi\sin\gamma) \qquad (14)$$

$$c' = V_1^4 \qquad (15)$$

The solution of (12) is:

$$P_2 = P_2^{cr} = \frac{-b' \pm \sqrt{b'^2 - 4a'c'}}{2a'} \qquad (16)$$

$$Q_2 = Q_2^{cr} = P_2^{cr} tg\phi \qquad (17)$$

The solution of (5) for $P_2 = P_2^{cr}$ and $b^2 - 4ac = 0$ on (10) gives:

$$V_2 = V_2^{cr} = +\sqrt{\frac{-b}{2a}} \qquad (18)$$

With the values of $P_2 = P_2^{cr}$ and $Q_2 = Q_2^{cr}$ founded analytically, it is possible to plot this boundary point on the *P-Q* Plane for each load power factor considered. Tables I and II summarize the critical values obtained from (12), (5) and (10) respectively. The powers are represented on 100 MVA base.

TABLE I
Operation of bus 2 at 1st and 4th quadrants

$\vec{S}_2$	ϕ (degree)	$tg\phi$ (rad)	$\cos\phi$ (rad)	V_2^{cr} (p.u.)	P_2^{cr} (p.u.)	Q_2^{cr} (p.u.)
I	36.87	0.75	0.80	0.6139	2.564	1.923
I	25.84	0.4843	0.90	0.6436	3.169	1.535
I	0.00	0.00	1.00	0.7558	4.857	0.000
IV	-18.19	-0.3286	0.95	0.8931	6.444	-2.117

TABLE II
Operation of bus 2 at 2nd and 3rd quadrants

$\vec{S}_2$	ϕ (degree)	$tg\phi$ (rad)	$\cos\phi$ (rad)	V_2^{cr} (p.u.)	P_2^{cr} (p.u.)	Q_2^{cr} (p.u.)
II	143.13	-0.75	-0.80	0.6497	-2.871	2.153
II	154.16	-0.4843	-0.90	0.6909	-3.653	1.769
II	180.00	0.00	-1.00	0.8465	-6.093	0.000
III	198.19	0.3286	-0.95	1.0445	-8.811	-2.895

C. P-Q Curves Simulation

Figure 9 shows the P-Q curves to the stable region of the voltage stability limit, obtained by the proposed method at the load bus 2, with addition of wind power generation. This situation can produce reverse power flow when the wind power generation is greater than the local load power. The P-Q plane shows the load bus receiving inductive reactive power at the first and second quadrants and receiving capacitive power at the third and fourth quadrants. The reverse power flow, where the system receives active power from the wind power, is showed at the second and third quadrants.

Figure 9 shows that the analytical solution and the simulation results are very close in the voltage stability limits. The security operation region is plotted for voltages at bus 2 considering the operational limits of 0.90 to 1.10 per unit. It can be seen that leading load power factor, makes the voltage stability limits and the secure voltage region in P-Q plane very close, as it was observed before in P-V curves of Figure 7.

The analytical solution is limited to very simple systems, and cannot be applied in a large and interconnected power system. The methodology that follows is generic and can be applied at any power systems.

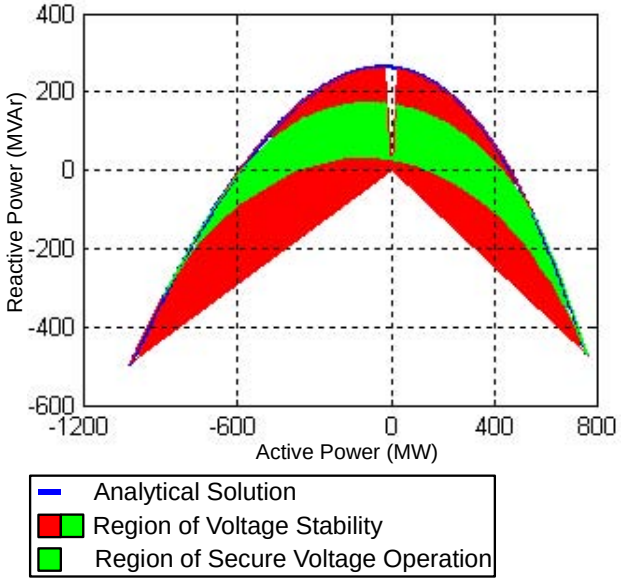

Fig. 9. Voltage stability regions in *P-Q* Plane.

IV. APPLYING THE PROPOSED METHOD ON DISTRIBUTION SYSTEM

The *P-Q* curves were constructed for a distribution system given on reference [8] showed in Appendix. The loads are increased with steps of 0.5%. The limits of the safe voltage in distribution buses are 0.95 to 1.05 per unit. The voltage stability limit and the secure operation voltage at bus 8 is analyzed considering four different scenarios in the system:

1. There is no wind power generation. The swing bus is a unique source of power.
2. The wind power generation is connected and operates as a *P-Q* bus with unit power factor.
3. The wind power is represented by a *P-V* bus with reactive power limits.
4. There is no wind or the wind velocity is to low to produce active power, so the converter produce only reactive power.

A. The Power System Limits

Figure 10 shows that the presence of wind power increases the stability limits. The load power factors are in the range of 0.8 inductive to 0.95 capacitive. The scenario where the wind power operates with zero power factor is beyond the limits of Figure 1. However, the requirements of the Electricity Supply Board National Grid in Ireland (ESBNG) is less restrictive with respect to wind reactive power generation limits. Note that, even if the wind speed is bellow the cut-in value the converters can still generate reactive power to improve the voltage stability margin and the region of safe voltage operation.

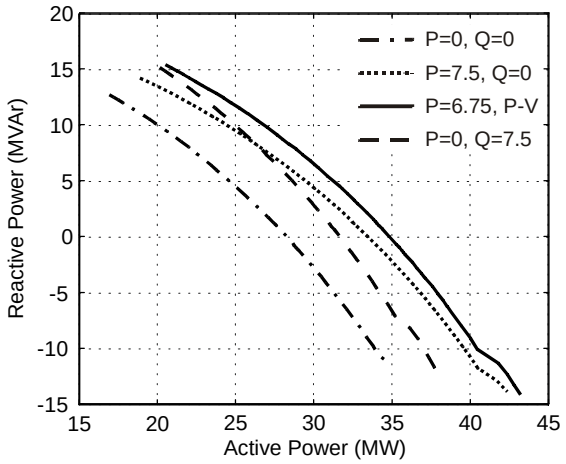

Fig. 10. Voltage stability limits on P-Q plane.

Figure 11 shows the regions of operational limits of voltage at bus 8 that is the operation points where the voltages are in the range of 0.95 to 1.05 per unit. The simulations are performed by using the similar algorithm as reference [8].

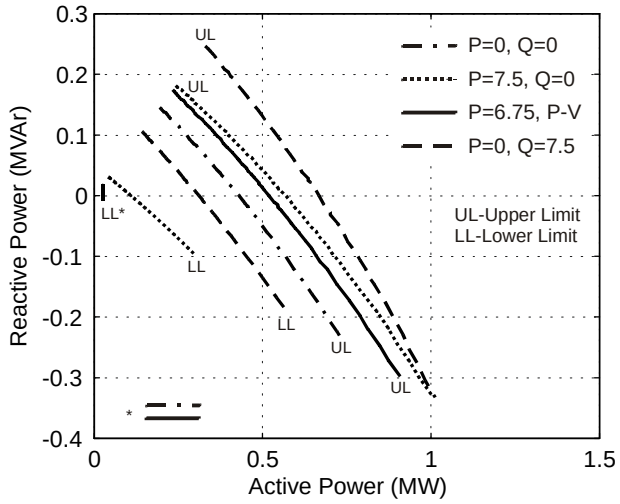

Fig. 11. Regions of secure voltage operation limits at bus 8

B. The Wind Power and Converter Capabilities Limits

Fig. 12 shows the P-Q curves for wind power at bus 12, the PCC of the wind farm, considering simultaneously the wind power and converter capability and power system limits. The load system was considered constant and the wind power generation varies with steps of 0.5%. It can be seen that the gray area is a secure voltage operation region that is common to power system and wind power generation. Note that this region is also limited by thermal current of the converter. This area contains the combination of powers that the wind power can operate and producing secure voltage operation. The others operation points of the wind turbine are restringing by the limitations imposed by the power system. With the enlarging of the reactive region of operation of the wind farms, that is changing his operational characteristic, it is possible to the PCC to operate in an enlarger region with secure voltage operation.

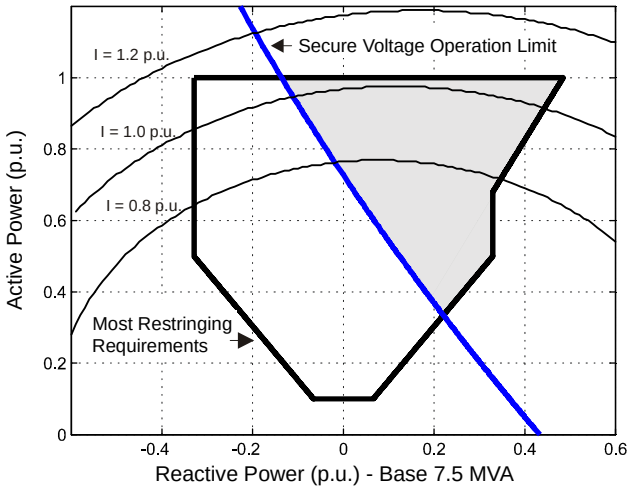

Fig. 12 Wind power capabilities and power system secure voltage operation limit.

It can be seen in Figure 12 that the wind power producing reactive power, the voltage remains within acceptable values and it produces and increasing in the power system voltage stability limit as showed in Figure 10.

V. CONCLUSION

A very efficient method is presented to determine the impact of the wind power generation on the steady-state voltage stability of a distribution power system. It is determined the security operation points of wind turbines, considering their requirements capabilities and power system limits.

To ensure the reliability of the results, a comparison between the proposed and a previous analytical method is carried out in a simple two bus system connected by a single transmission line.

The voltage stability limit region and a sub-region in which the voltages at the bus are in acceptable ranges are defined for different power factors. For practical purposes, the *P-Q* curves can be useful to determine the capacity of certain buses of the system to support an increasing in the load demand. Of course, to meet de new demand, the limits of secure voltages must be determined. *P-Q* curves can help the utilities in the choice the best point to connect the wind farms. It is demonstrated that the wind power capability limits can impose operational restrictions to the power system voltage stability limits.

APPENDIX

Figure A1 shows the simplified diagram of test system. It has 20 buses operating at the voltage of 12.47 kV, 19 circuits/transformers, and the hypothetical wind power is connected at bus 20 at 0.69 kV. The detailed of transmission system is not showed but it has only one circuit of 138 kV. The power wind farm is a variable speed direct-drive synchronous generator connected to the PCC by a full-load converter. The distribution line parameters and the power flow data can be found in [8].

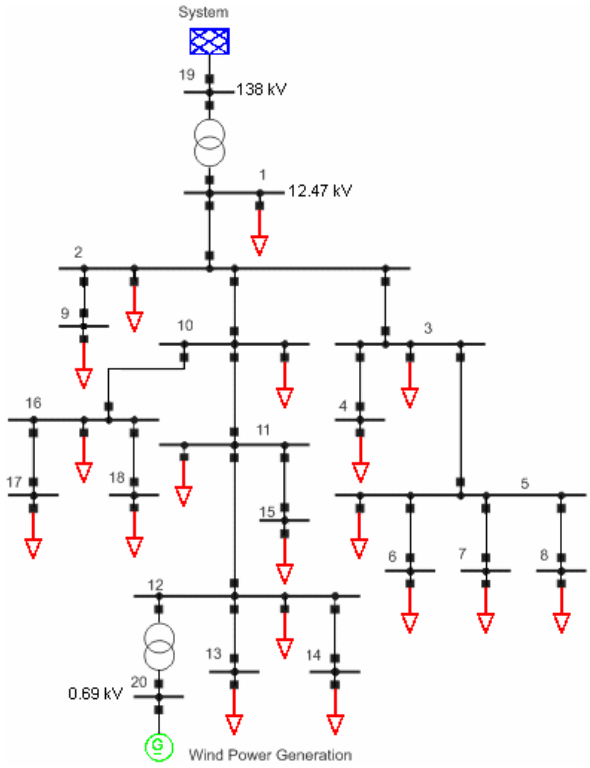

Fig. A1. Distribution Power System Test.

ACKNOWLEDGMENT

This paper is part of a Project of Research & Development n° 9928180 with the Universidade Federal de Santa Maria – UFSM and the Companhia Estadual de Distribuição de Energia Elétrica – CEEE-D. The authors gratefully acknowledge the financial support from UFSM and CEEE-D.

REFERENCES

[1] R.K.Gupta, Z.A.Alaywan, R.B.Stuart and, T.A.Reece: Steady State Voltage Instability Operations Perspective, *IEEE Trans. on Power System.*, Vol. 5, pp. 1345-1351, 1990.

[2] C. L. Masters: *V*oltage Rise the Big Issue when Connecting Embedded Generation to Long 11 kV Overhead Lines, *Power Engineering Journal*, February 2002.

[3] M.H. Haque: Determination of Steady-State Voltage Stability Limit Using P-Q Curve, *IEEE Power Engineering Review*, April 2002.

[4] P.Kundur: Power: *System Stability and Control*, New York: McGraw-Hill, 1994.

[5] F.W. Mohn, C. Z. de Souza: Tracing PV and QV Curves with the Help of a CRIC Continuation Method, *IEEE Trans. on Power System.*, Vol. 21, Nº 3, pp.1115-1122, 2006.

[6] W. Christiansen, D. T. Johnsen: Analysis of requirements in selected Grid Codes, *Section of Electric power Engineering*, Technical University of Denmark, January 2006.

[7] M. Chinchilla, S. Arnalte, J.C. Burgos, and J.L. Rodríguez: Power limits of grid-connected modern wind energy systems, *Renewable Energy*, September 2005, pp. 1455-1470.

[8] L. Mariotto, H. Pinheiro, G. Cardoso Junior, M.R. Muraro: Determination of the Static Voltage Stability Region of Distribution Systems with the Presence of Wind Power Generation, *International Conference on Clean Electrical Power*, May 2007, Capri – Italy, 556-562.